

December 9, 1996

OCAN129601

U. S. Nuclear Regulatory Commission
Document Control Desk
Mail Station P1-137
Washington, DC 20555

Subject: Arkansas Nuclear One - Units 1 and 2
Docket Nos. 50-313 and 50-368
License Nos. DPR-51 and NPF-6
Additional Information Regarding Technical Specifications Change
Request to Delete Reactor Coolant Pump Flywheel Inspections

Gentlemen:

By letter dated April 4, 1995 (OCAN049504), Entergy Operations requested changes to the Arkansas Nuclear One, Units 1 and 2 (ANO-1 and 2) Technical Specifications. The changes were to delete the requirements for inservice inspections of reactor coolant pump (RCP) flywheels. ANO submitted the proposed changes as a lead plant for the Combustion Engineering Owners Group. The other affected plants are Millstone-2, Palisades, St. Lucie Units 1 and 2, and Waterford 3.

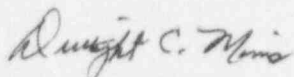
The staff informed ANO that the generic implications of the total deletion of the flywheel inspections could not be resolved prior to ANO's next scheduled flywheel inspection (ANO-2 refueling outage 2R11). In order to obtain relief for the next inspection, Entergy Operations submitted a revised Technical Specification Change Request (TSCR) on August 25, 1995 (2CAN089505). The NRC granted the relief in a letter to ANO dated September 22, 1995 (2CNA099507).

Entergy Operations submitted a similar revised TSCR for ANO-1 on August 23, 1996 (1CAN089602), since ANO was informed by the NRC that the generic implications of the total deletion of the flywheel inspections could not be resolved prior to ANO-1's next scheduled flywheel inspection (refueling outage 1R13). This request for relief was withdrawn via correspondence to the NRC dated October 9, 1996 (1CAN099602). The flywheels were inspected during refueling outage 1R13. The results of these inspections indicated no flaws or cracks. The results were provided to the NRC staff in a letter dated November 20, 1996 (1CAN119603), to provide further data in support of the original (April 5, 1995) TSCR to completely eliminate RCP flywheel inspections.

In a letter dated October 2, 1996 (OCNA109601), the NRC staff requested additional information in order to complete their review of the original TSCR. The additional information is provided in the attachment.

Should you have further questions, please contact me.

Very truly yours,



Dwight C. Mims
Director, Nuclear Safety

DCM/dwb

Attachment

cc: Mr. Leonard J. Callan
Regional Administrator
U. S. Nuclear Regulatory Commission
Region IV
611 Ryan Plaza Drive, Suite 400
Arlington, TX 76011-8064

NRC Senior Resident Inspector
Arkansas Nuclear One
P.O. Box 310
London, AR 72847

Mr. George Kalman
NRR Project Manager Region IV/ANO-1 & 2
U. S. Nuclear Regulatory Commission
NRR Mail Stop 13-H-3
One White Flint North
11555 Rockville Pike
Rockville, MD 20852

Response to Questions Related to "Relaxation of Reactor Coolant Pump Flywheel Inspection Requirements"

- 1. Section 3.0, Previous Inspection Results for RCP [Reactor Coolant Pump] Flywheels, Pgs. 3-1 to 3-12: Provide additional information if the ultrasonic (UT) examinations at the Combustion Engineering Owners Group (CEOG) member plants were qualified relative to inspection of RCP flywheels. Regardless whether a formal qualification was performed, please include in your response the following:**

Note: Inspection related questions 1 and 2 are answered from the perspective of the lead CEOG plant, Arkansas Nuclear One, Units 1 and 2 (ANO-1 and 2). The flywheel inspection program at ANO is considered representative of the inspection programs in existence at the other CEOG member plants.

- a. Any information supporting qualification of the examinations of RCP flywheels.**

At this time, there has not been any "formal" qualification of the ultrasonic (UT) techniques used for examination of the RCP flywheels at ANO. The techniques utilized at ANO are consistent with the techniques used at other plants throughout the industry. The techniques generally consists of using a calibrated metal path to detect the keyway in the flywheel or a notch in a block, adding gain, and scanning for the appearance of any uncharacteristic reflectors that are not indicative of the geometry of the bore/keyway or holes in the flywheel.

- b. Any information supporting qualification of the personnel performing the examinations of RCP flywheels.**

Ultrasonic examination personnel that have performed the RCP flywheel examinations were all certified to Level II or Level III. Some of the examination personnel also held EPRI Intergranular Stress Corrosion Cracking (IGSCC) or Performance Demonstration Initiative (PDI) detection certifications. Examination personnel utilized in the past have not been specifically qualified to examine RCP flywheels via a performance demonstration.

- c. Any information regarding the degree of uncertainty in UT measurements based on the procedures and personnel qualification basis.**

At this time, it is uncertain how capable any of the examination techniques currently used would be for sizing an indication after detection. The techniques can provide confirmation of the absence or presence of flaws but may not be effective for measuring dimensions of a detected flaw.

2. **Section 3.0, Previous Inspection Results for RCP Flywheels, Pgs. 3-1 to 3-12:** The fatigue analysis is dependent on the premise that UT equipment used for examinations of RCP flywheels at these facilities is capable of accurately detecting and sizing a 0.25-inch long near-surface flaw. Provide your basis supporting the probability of detection (POD) for the examinations performed. Provide details on how the POD values were determined, qualified, and used in concluding the assumed size of the initial flaw. Also, provide a demonstration of the CEOG member plants' UT detection capability in not missing a flaw size of 0.25 inch.

As stated in response to question 1 above, there has been no formal qualification of the UT procedures on known or "mock" flaws. The procedures were based on generic UT principles.

Previous ultrasonic technique qualifications for probability of detection of a given flaw was considered in determining the 0.25 inch minimum detectable size flaw. The flaw size generally agreed upon by the participating utilities as being reasonably detectable was 0.25 inch. Guidance was also taken from the ANO-1 Safety Analysis Report, which references ASME Section III (Class A N-321 and N-322) requirements that state that the smallest radial crack that could exist in a plate having passed an angle beam UT examination would be less than 0.24 inch based on a plate thickness of eight inches and a three percent notch.

Even though a detectable flaw size minimum has not been proven by mock-up performance demonstrations, ANO has conducted an evaluation of detectability on known notches in a calibration block.

ANO calibration block UT-99 is a 6.125 inches thick block that has several mock keyways that are 1 inch deep by either 1 inch or 3 inches in width. There are a series of machined notches in the keyways that are either 0.100 inch or 0.400 inch in depth. An exercise was conducted using the ultrasonic techniques used to examine the flywheels at ANO-1 and 2. Using each technique separately, both the 0.100 inch and 0.400 inch notches were detectable in at least one direction of scanning. The 0.100 inch notch was difficult to separate from the keyway corner signal, but could be seen as a moving signal directly in front of the upper corner signal. The 0.400 inch notch was readily detectable with all techniques used.

Even though this exercise does not define an absolute minimum detectable value, it does bound a detectable flaw size value between 0.100 inch and 0.400 inch. Based on this, it would seem reasonable that an 0.25 inch flaw would have a good probability of detection, depending on the orientation of the flaw and the direction of the scan.

Furthermore, an evaluation was performed to determine the acceptable initial flaw size that can be tolerated by the flywheels with consideration of crack growth. In this

crack growth evaluation, 4000 cycles were assumed (eight times the 500 cycles for plant life defined in the plants' technical specifications). A summary of this evaluation is presented below in Table 1 for all flywheels. For the most limiting case, the acceptable initial flaw size is more than double the originally assumed 0.25 inch. This effectively renders the detection capability of a 0.25 inch flaw moot. The question now becomes, can a flaw greater than 0.5 inch be reliably detected?

If the NRC believes a performance demonstration of this capability is still warranted, the CEOG will gladly comply, but will need to address some issues, e.g., flaw size, implanted fatigue crack or electrodischarge machining (EDM) notch, with the staff before a mockup is fabricated for this purpose.

Table 1
Acceptable Initial Flaw Sizes

Plant Name	Allowable Flaw Size	Acceptable Initial Flaw Size Considering Crack Growth
ANO-1	1.16	1.148
ANO-2	>2	>2
Millstone-2	>2	>2
Palisades	>2	>2
St. Lucie 1 & 2	>2	>2
Waterford-3	0.58	0.579

3. **Section 6.1.1, Centrifugal Stresses, Pg. 6-1:** It was stated in curve-fitting the stress distribution that a radial distance of 2 inches from the keyway was considered in order to obtain an accurate fit. Did you only consider the stress distribution within this 2-inch range in the fracture mechanics analysis or did you exclude this part of stress distribution in your analysis?

Only the stress distribution within the 2-inch radial distance from the keyway was used for the curve fit and thus considered in the fracture mechanics evaluation. As can be seen from Figures 6-3 through 6-14 in the subject report, the stress intensity factor was only calculated within this 2-inch distance. This approach is consistent with current ASME Section XI evaluation methodology (1992 Edition) which specifies curve fit over the crack depth.

4. **Section 6.1.1, Centrifugal Stresses, Pg. 6-1: The finite element method (FEM) was employed in the stress analysis, but not in the fracture mechanics analyses. Support your fracture mechanics results by modifying the FEM model to include the postulated crack and then input the crack face pressure using the complete tangential stress distributions for the critical keyway regions in Figures 5-28 through 5-33 or demonstrate that the simplified models used are conservative.**

In the subject report, a model consisting of a longitudinal crack in the cylinder with $t/R = 1.2$ (t : thickness and R : inside radius) was chosen for the large-bore flywheels at ANO-1, Palisades, and St. Lucie Units 1 and 2. For the smaller bore flywheels at ANO-2, Millstone-2, and Waterford-3, a model consisting of a crack emanating from a hole in an infinite plate was chosen. To show the adequacy in the use of these models, sensitivity studies were performed to determine the effect of the geometric parameter, t/R , ranging from 0.1 to infinity. This was achieved by using various models from the *pc-CRACK* software library.

The analysis was performed for all the large-bore and small-bore flywheels for the plants considered in the subject report. The results of the evaluation in terms of stress intensity factor, K , versus crack length are presented in Figures 1 through 6.

For the large-bore flywheels of ANO-1, Palisades, and St. Lucie 1 and 2, the K variation with flaw length does not change significantly between the various t/R ratios for crack lengths up to about 1 inch as shown in Figures 1 through 3. The actual t/R ratios for these flywheels varies from 1.22 to 1.37, as shown in Table 2. In the subject report, a t/R ratio of 1.2 was used to perform the evaluation which, for analysis purposes, is slightly more conservative than the actual t/R values for these large-bore flywheels shown in Table 2. Hence, the results presented in the subject report are conservative.

The K versus flaw size distributions for the small-bore flywheels are shown in Figures 4 through 6 for ANO-2, Millstone-2, and Waterford-3. The actual t/R ratios for these flywheels vary from 4.46 to 4.93 as shown in Table 2. In the evaluation in the subject report, a crack emanating from a hole in an infinite plate with t/R of infinity was used. This model, although slightly less conservative than the actual t/R values for the flywheels for crack lengths greater than 0.75 inches, is acceptable considering the relatively large t/R ratios of these flywheels. To determine the sensitivity of the t/R ratio, the allowable flaw sizes were calculated using both models with t/R values of 1.2 and infinity, as explained in Item 5 below, even though it is believed that the t/R ratio of infinity more closely represents these small-bore flywheels. Both models yielded acceptable results.

Table 2
Geometric Data and t/R Ratios for Flywheels

Plant Name	Bore Diameter (in.)	Outside Diameter (in.)	Thickness t (in.)	Inside Radius (R) (in.)	t/R
ANO-1	30.4	72.0	20.80	15.2	1.37
ANO-2	13.74	81.5	33.88	6.87	4.93
Millstone-2	13.74	75.0	30.63	6.87	4.46
Palisades	33.0	72.0	19.50	15.5	1.25
St. Lucie 1 & 2	32.5	72.0	19.75	16.25	1.22
Waterford-3	13.75	78.0	32.125	6.875	4.67

LEFM Model Comparison Large Bore - ANO-1 (Centrifugal)

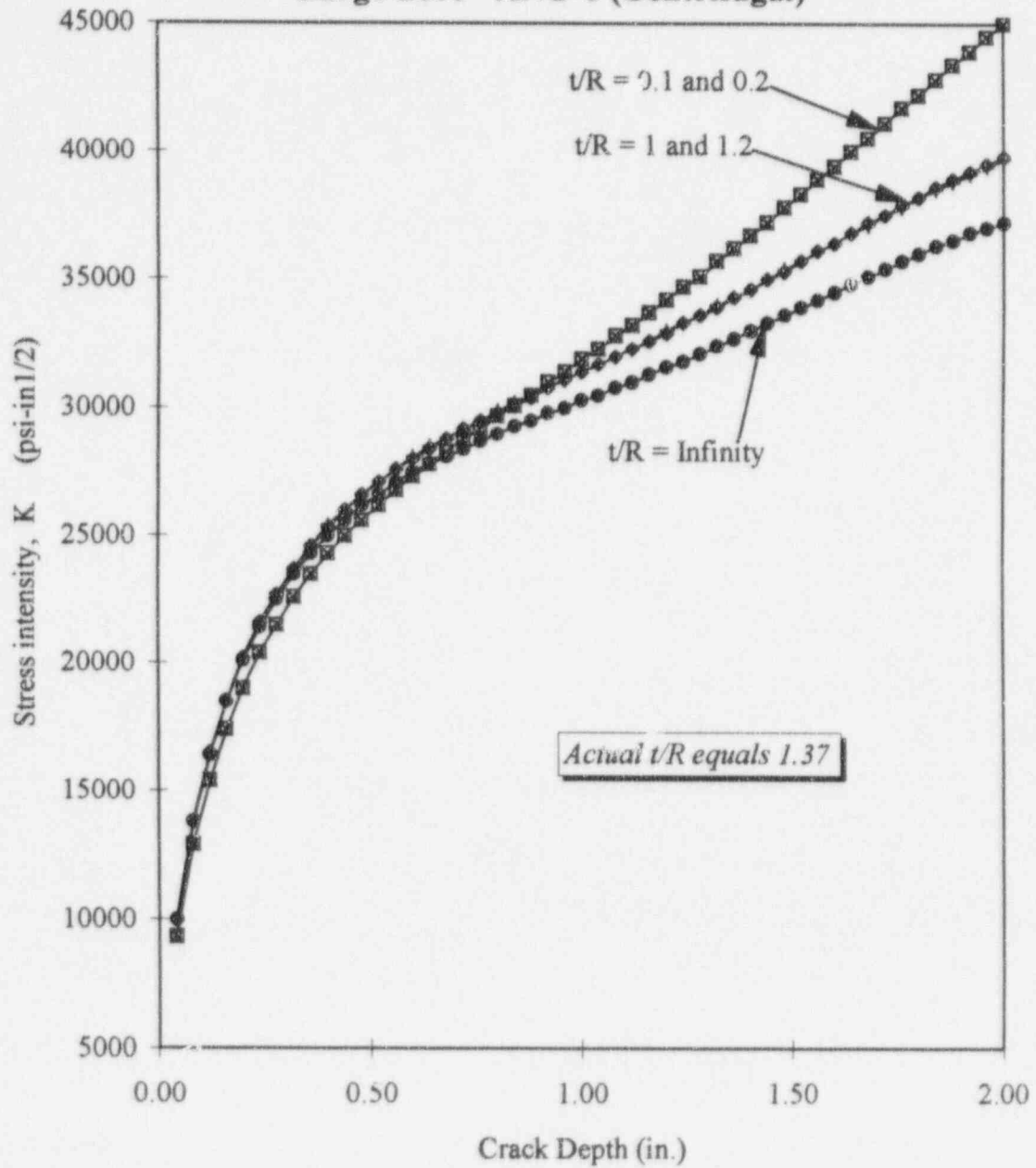


Figure 1. Comparison of Stress Intensity Factors for Various R/t Ratios - ANO-1

LEFM Model Comparison Large Bore - PALISADES (Centrifugal)

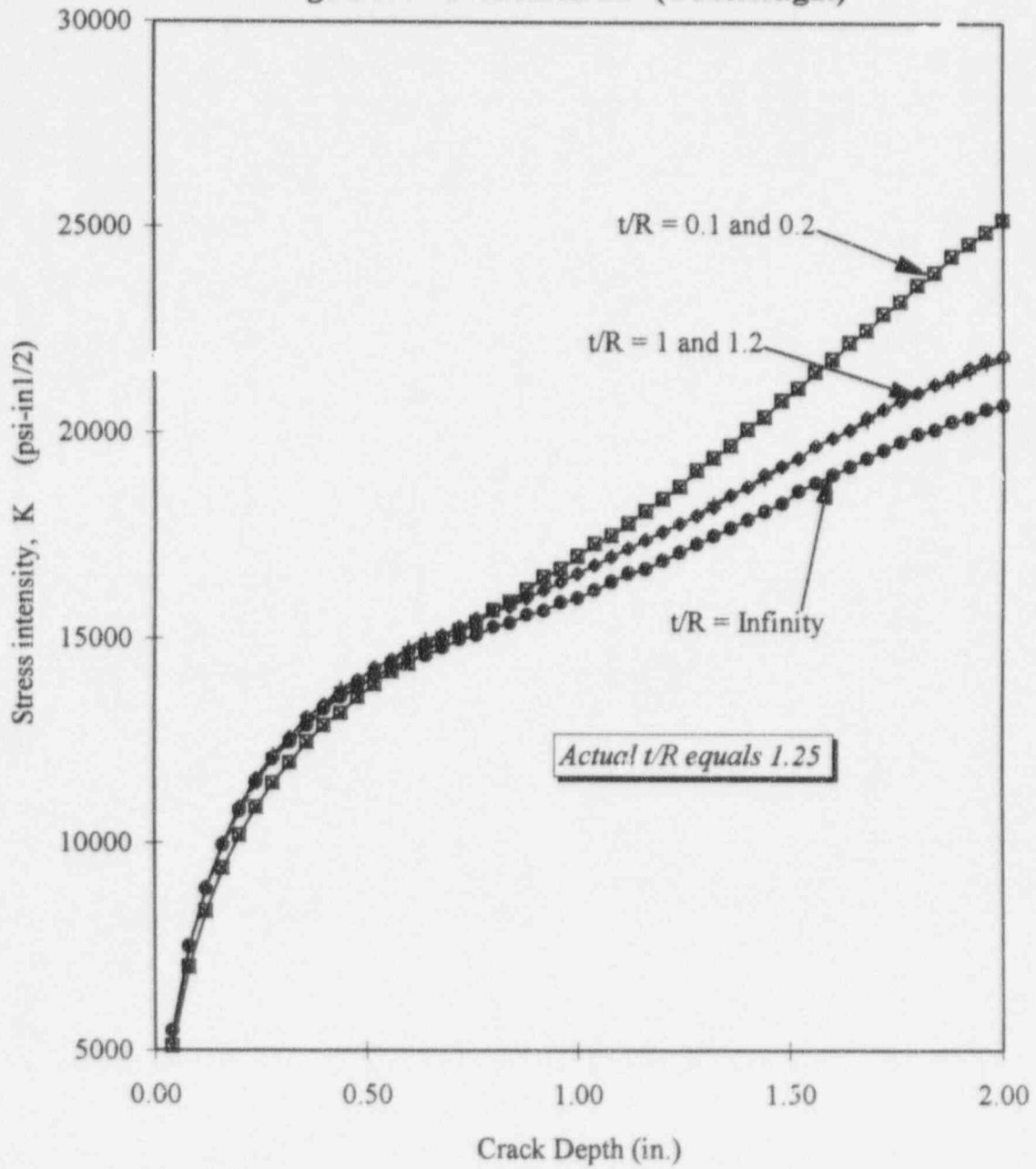


Figure 2. Comparison of Stress Intensity Factors for Various R/t Ratios - Palisades

LEFM Model Comparison Large Bore - ST. LUCIE (Centrifugal)

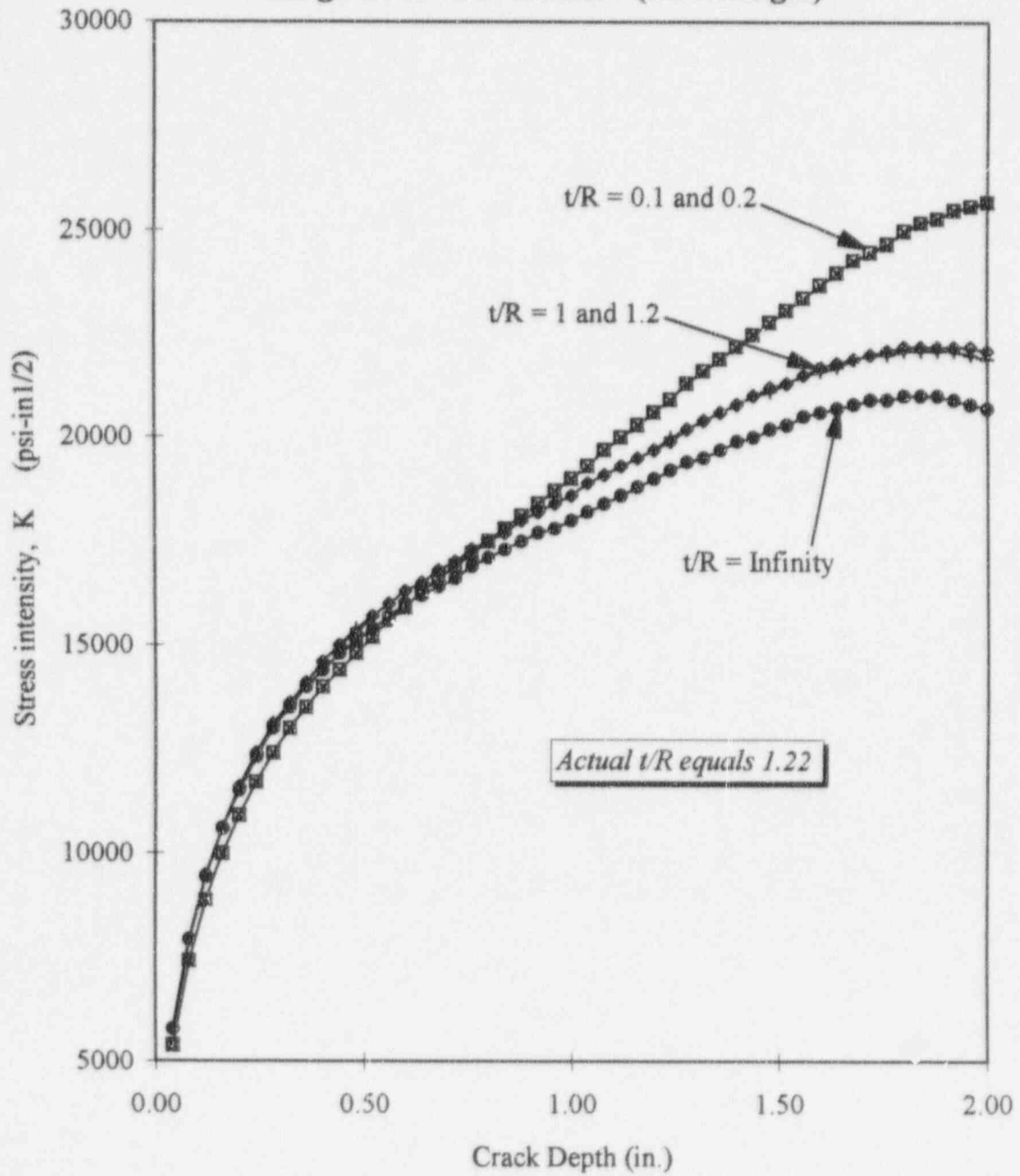


Figure 3. Comparison of Stress Intensity Factors for Various R/t Ratios- St. Lucie 1 and 2

LEFM Model Comparison Small Bore - ANO-2 (Centrifugal)

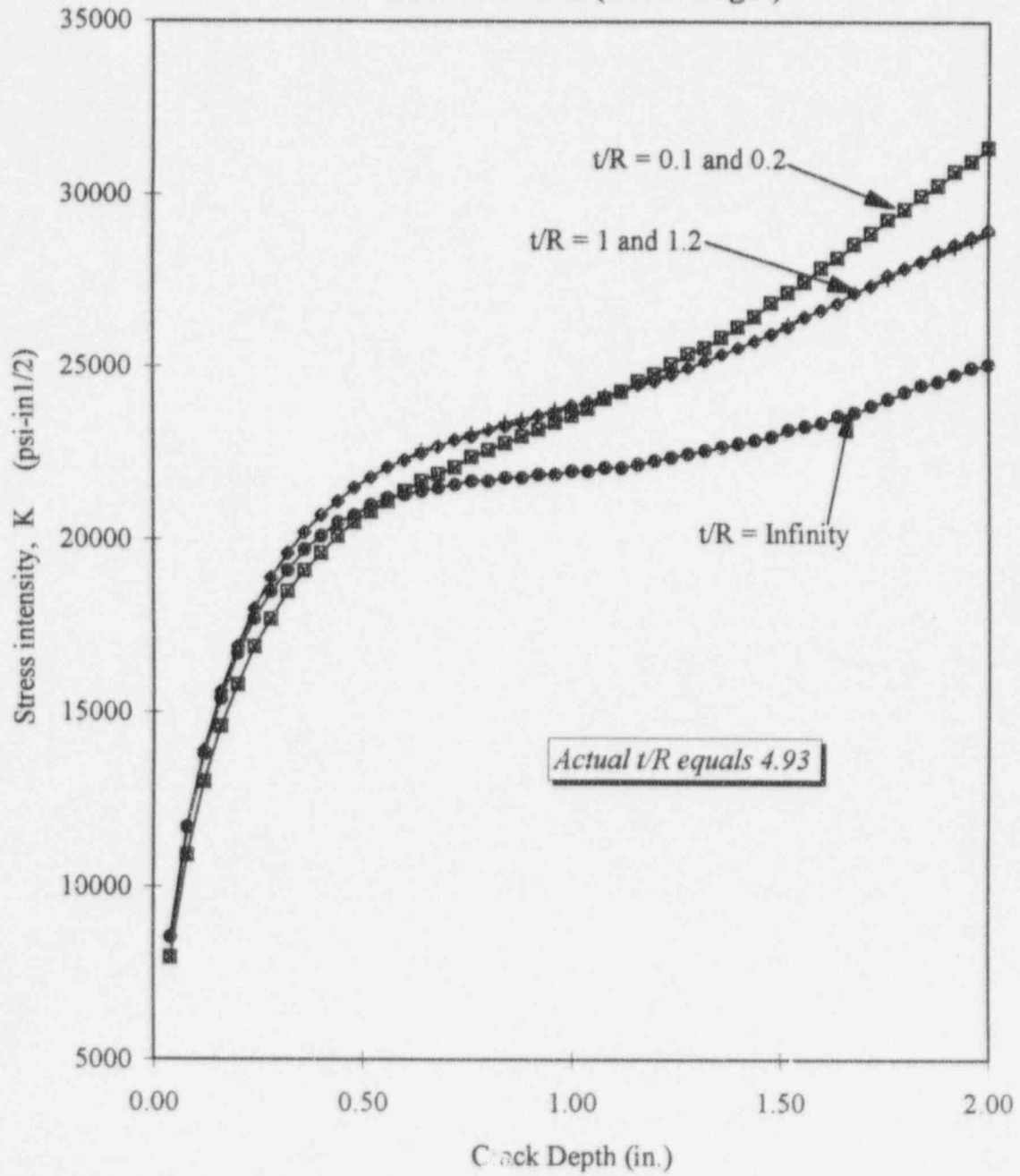


Figure 4. Comparison of Stress Intensity Factors for Various k/t Ratios - ANO-2

LEFM Model Comparison Small Bore - (Centrifugal) MILLSTONE

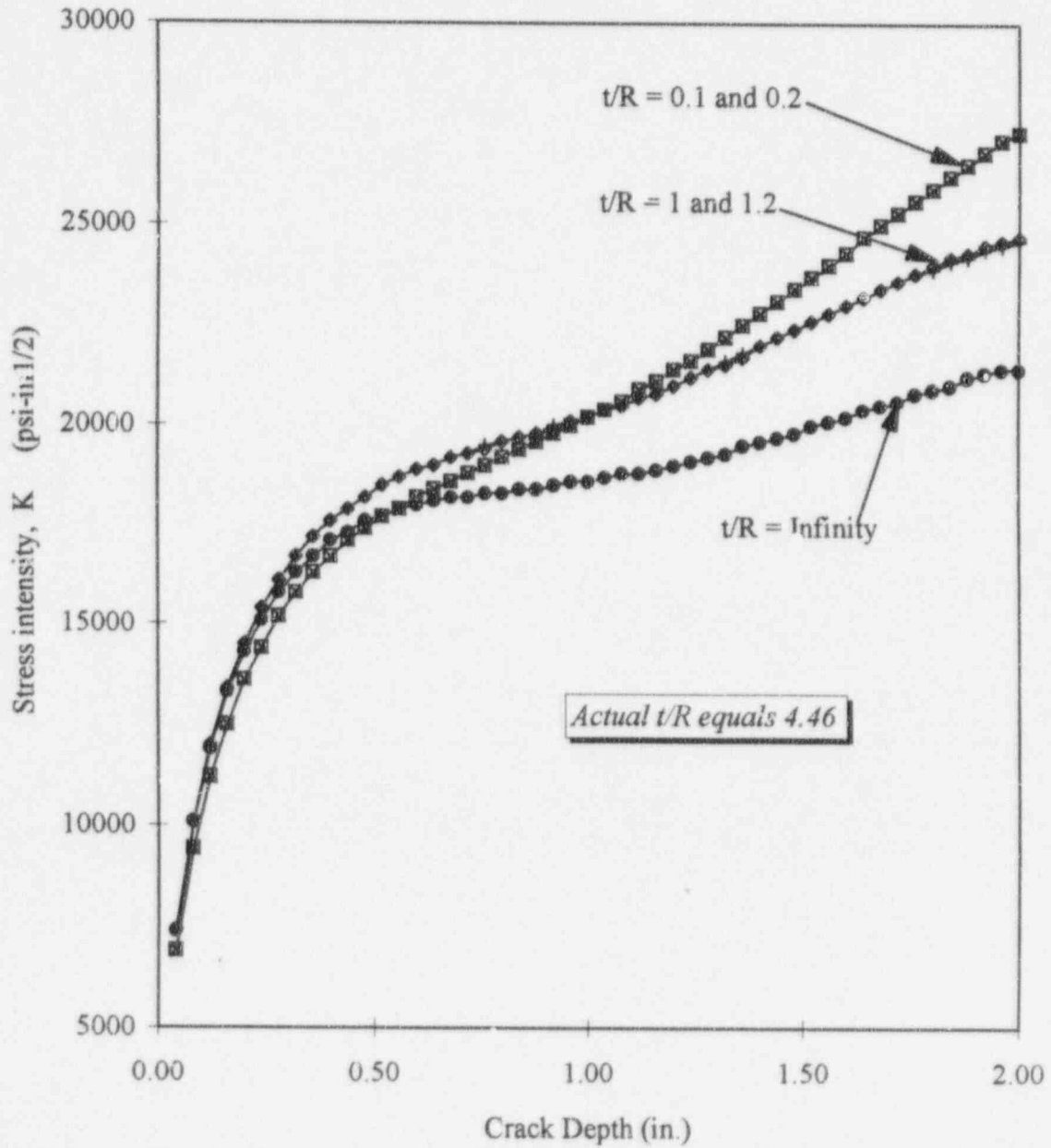


Figure 5. Comparison of Stress Intensity Factors for Various R/t Ratios - Millstone-2

LEFM Model Comparison Small Bore - (Centrifugal) WATERFORD

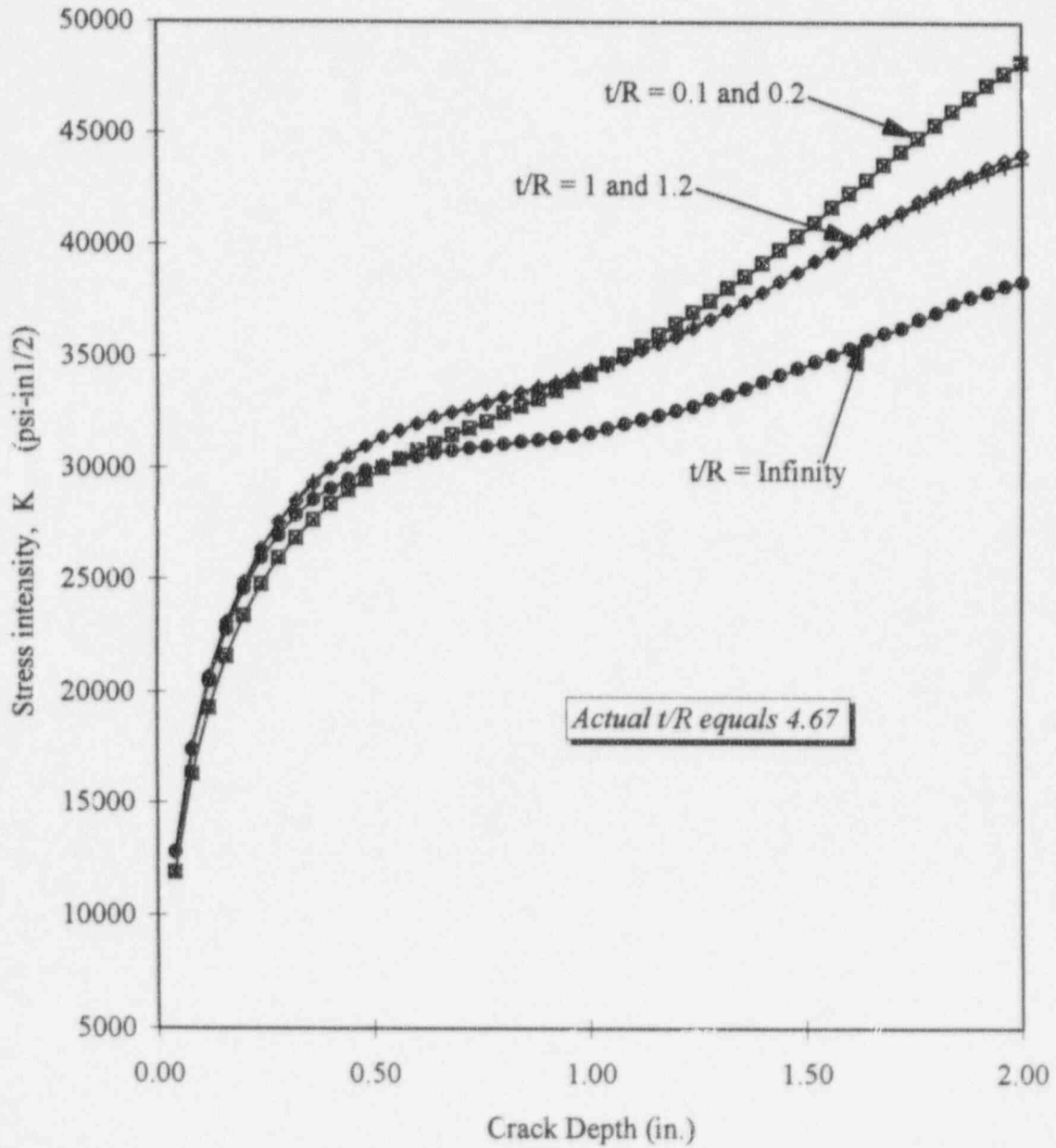


Figure 6. Comparison of Stress Intensity Factors for Various R/t Ratios - Waterford-3

5. **Section 6.3, Allowable Flaw Size Determination, Pg. 6-6:** It was stated that the stress intensity distribution for the centrifugal and the shrink-fit stresses are compared separately with the allowable fracture toughness to determine the allowable flaw sizes. Under normal operating conditions, the staff believes that contributions from both centrifugal and shrink-fit stresses to the applied stress intensity factors are comparable and should be combined. Figures 6-3 through 6-8 indicate that when the combined effect is considered the ASME Code criteria may not be met even for the initial crack size of 0.25 inch. Clarify this. Also, provide a revised copy of Figures 6-3 and 6-14 by adding the stress intensity due to shrink fit at the proper speed to the stress intensity due to centrifugal load.

In the subject report, the centrifugal and the shrink-fit stresses were treated separately to determine the allowable sizes since the maximum stresses for these two loads do not occur at the same time. This approach was considered reasonable since very conservative shrink-fit values were used in the analysis (5.2 mils for the small-bore flywheels and 12.5 mils for the large-bore flywheels). In addition, the shrink-fit stresses are secondary (displacement type) stresses whose contribution to fracture is not as significant as the primary centrifugal stresses. It is expected that because of the very conservative initial shrink-fit values assumed in the analysis, that some amount of shrink-fit will still be present at the normal operating speed of the flywheel.

To determine the residual shrink-fit values at normal operating speed, the finite element analysis performed in support of the subject report was reviewed to determine the relative displacement (initial shrink-fit minus centrifugal displacement) at normal operating speed. This relative displacement was used to calculate the residual shrink-fit stresses at normal operating speed. Stress intensity factors calculated for the centrifugal and residual shrink-fit stresses at normal operating speed are shown in Figures 7 through 15 for all the flywheels that were evaluated in the subject report. For the large-bore flywheels, a model with t/R ratio of 1.2 was used to calculate the applied stress intensity factor and is shown in Figures 7 through 9. For the small-bore flywheels, stress intensity factors were calculated using t/R ratios of 1.2 and infinity as shown in Figures 10 through 15.

To determine the allowable flaw size, a safety factor of 3, consistent with ASME Code Section XI, was applied to the centrifugal stresses since these are primary stresses. A safety factor of 1 was applied to the shrink-fit stresses since these are displacement type stresses which do not contribute to the fracture of the ductile materials. All the flywheels operate in the upper shelf region and are therefore expected to exhibit very ductile behavior. Precedent for the use of a safety factor of 1 for secondary stresses has been established in ASME Code, Section XI, Appendix C for materials that exhibit elastic-plastic fracture behavior. The comparison of the total factored applied stress intensity factors with the fracture toughness for the flywheels are shown in Figures 7 through 15. The allowable flaw sizes resulting from these comparisons are shown in Table 3.

It can be seen that these allowable flaw sizes are greater than the final flaw sizes for the assumed initial flaws of 0.25 inches in the flywheels, even when the conservative shrink-fit stresses are considered in the evaluation and, even if a conservative model with $t/R = 1.2$ is used for the small-bore flywheels. This demonstrates that the conclusions of the subject report are not changed by inclusion of the secondary shrink-fit stresses in the determination of the allowable flaw sizes.

Table 3
Allowable Flaw Sizes
Centrifugal + Shrink-Fit Stresses

Plant Name	Allowable Flaw Size	
	$t/R = 1.2$	$t/R = \infty$
ANO-1	1.16	N/A
ANO-2	1.60	>2
Millstone-2	1.48	>2
Palisades	>2	N/A
St. Lucie 1 & 2	>2	N/A
Waterford-3	0.43	0.58

Allowable Flaw Evaluation Normal Operating Conditions Large Bore Case - ANO-1

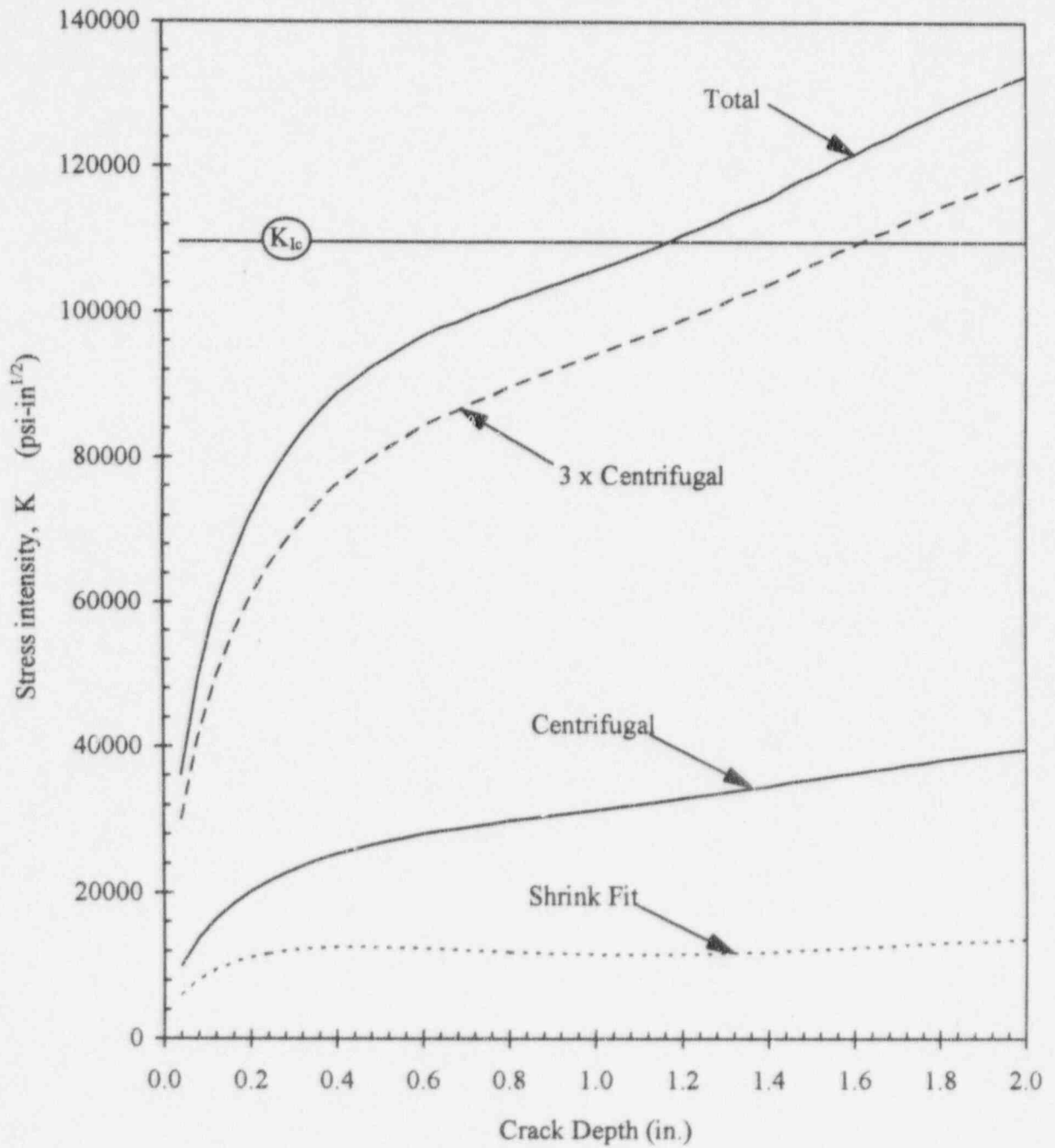


Figure 7 Determination of Allowable Flaw Size ($t/R = 1.2$) - ANO-1

Allowable Flaw Evaluation Normal Operating Conditions PALISADES

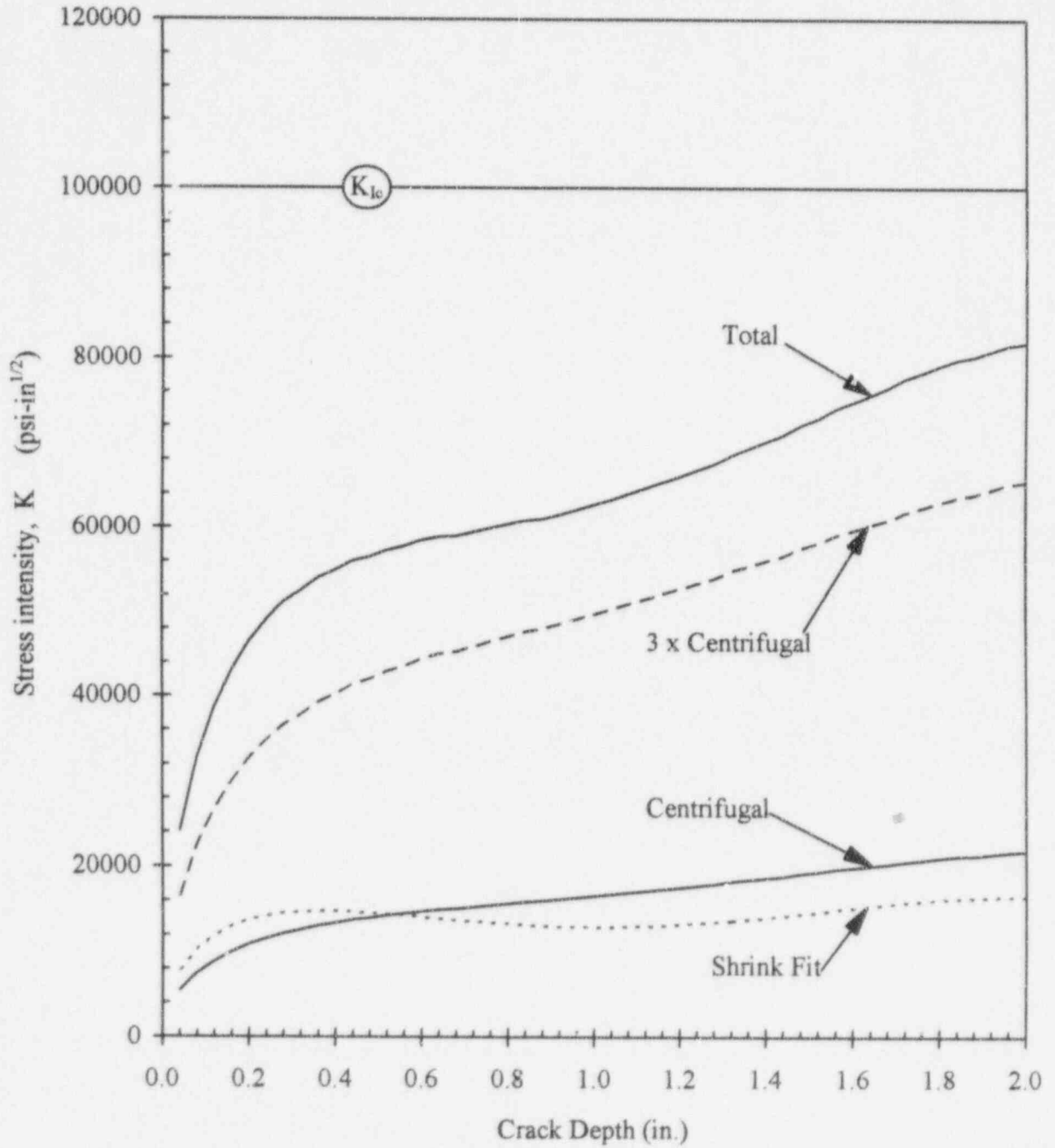


Figure 8. Determination of Allowable Flaw Size ($t/R = 1.2$) - Palisades

Allowable Flaw Evaluation Normal Operating Conditions ST. LUCIE

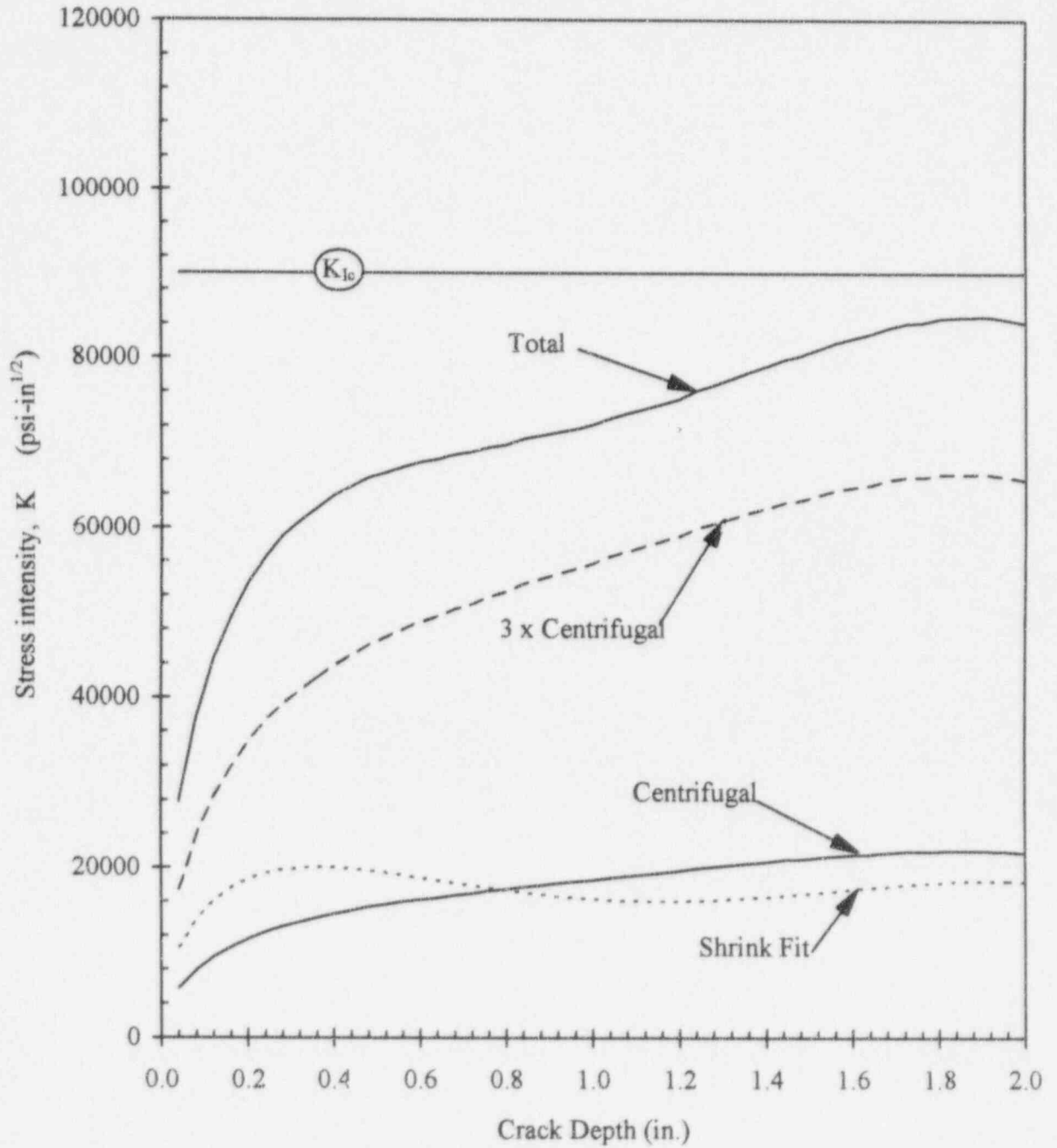


Figure 9. Determination of Allowable Flaw Size ($t/R = 1.2$) - St. Lucie 1 and 2

Allowable Flaw Size Evaluation Normal Operating Conditions Small Bore - ANO-2

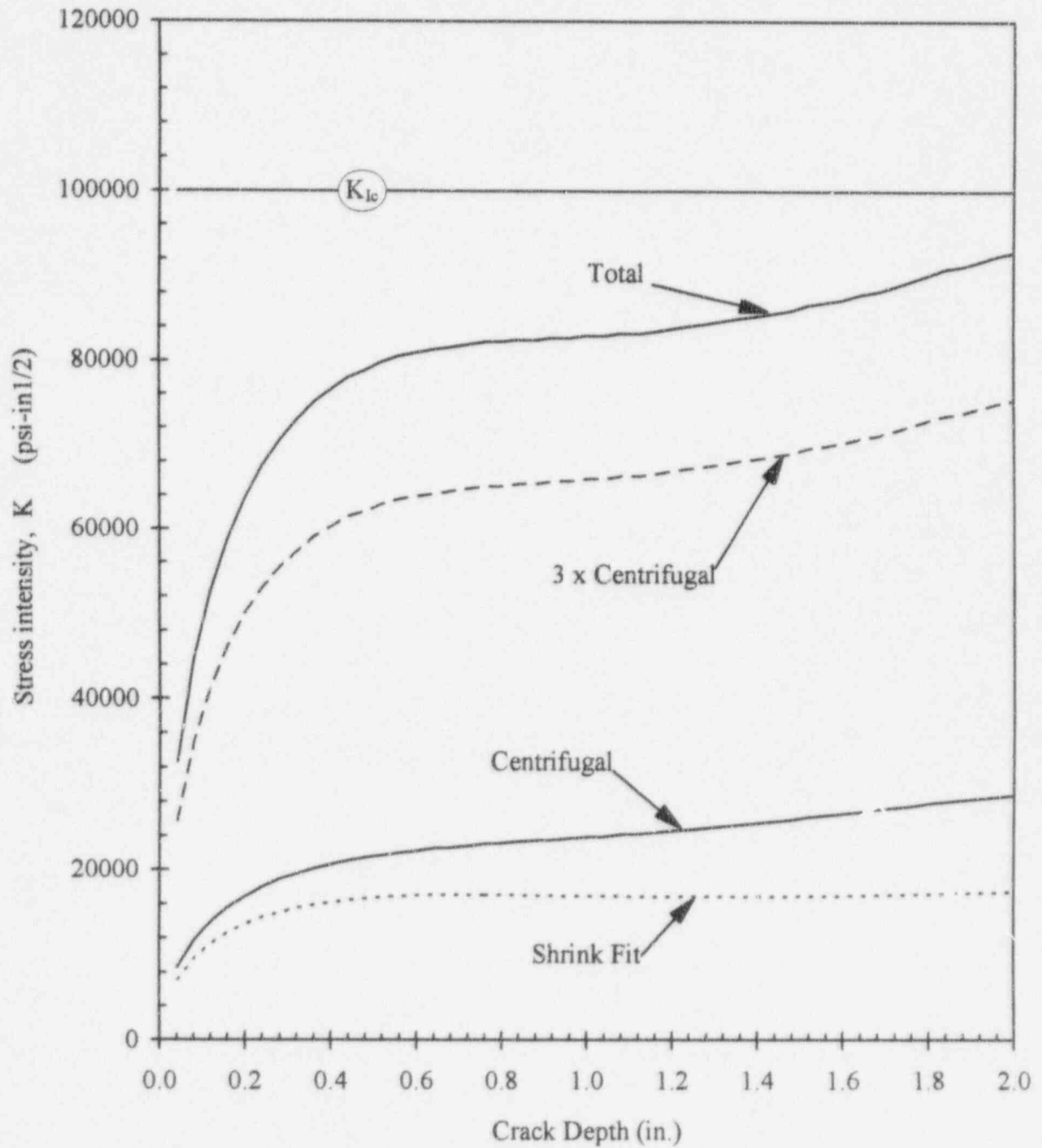


Figure 10. Determination of Allowable Flaw Size ($t/R = \infty$) - ANO-2

Allowable Flaw Size Evaluation Normal Operating Conditions MILLSTONE

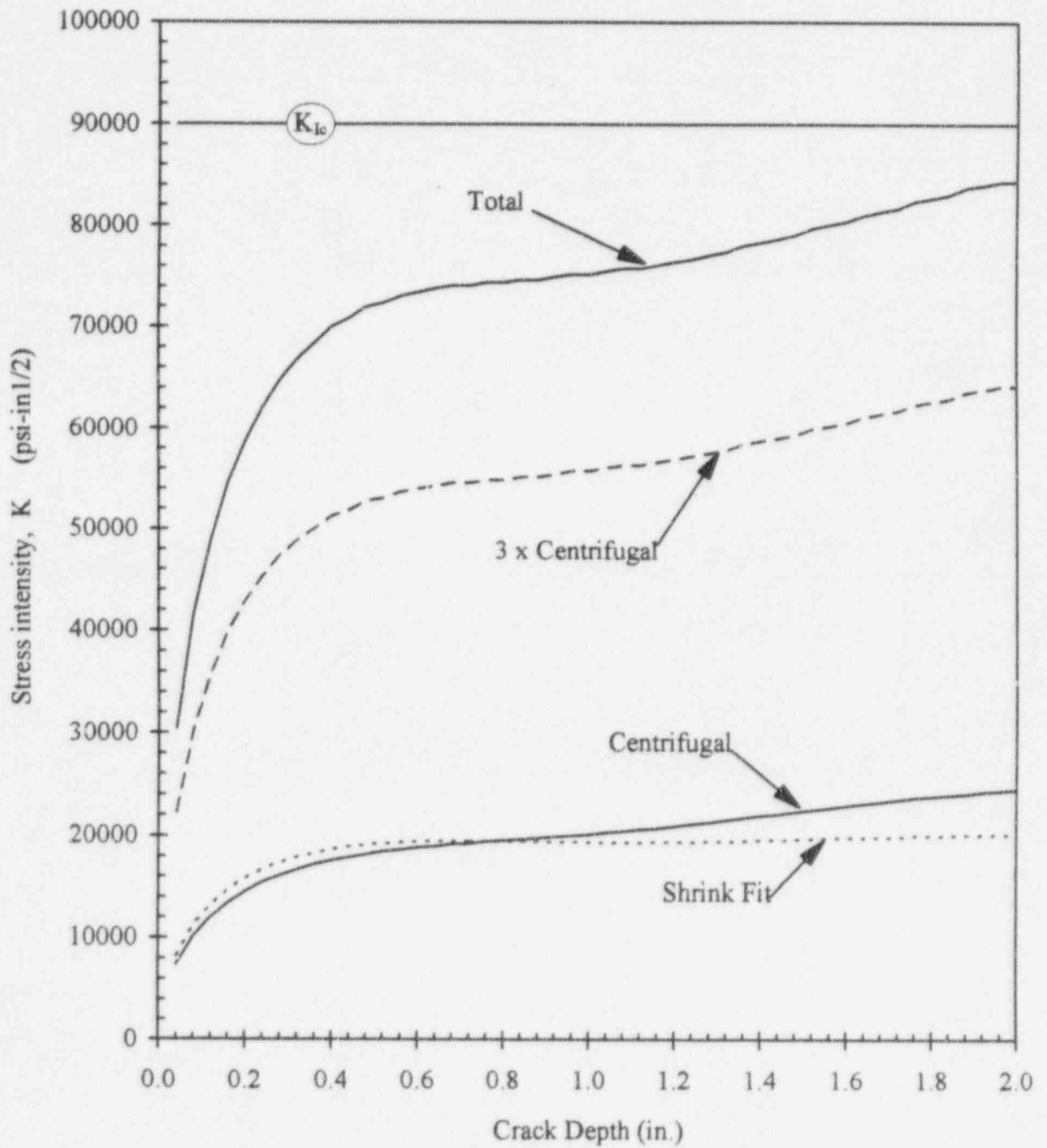


Figure 11. Determination of Allowable Flaw Size ($t/R = \infty$) - Millstone-2

Allowable Flaw Size Evaluation Normal Operating Conditions WATERFORD

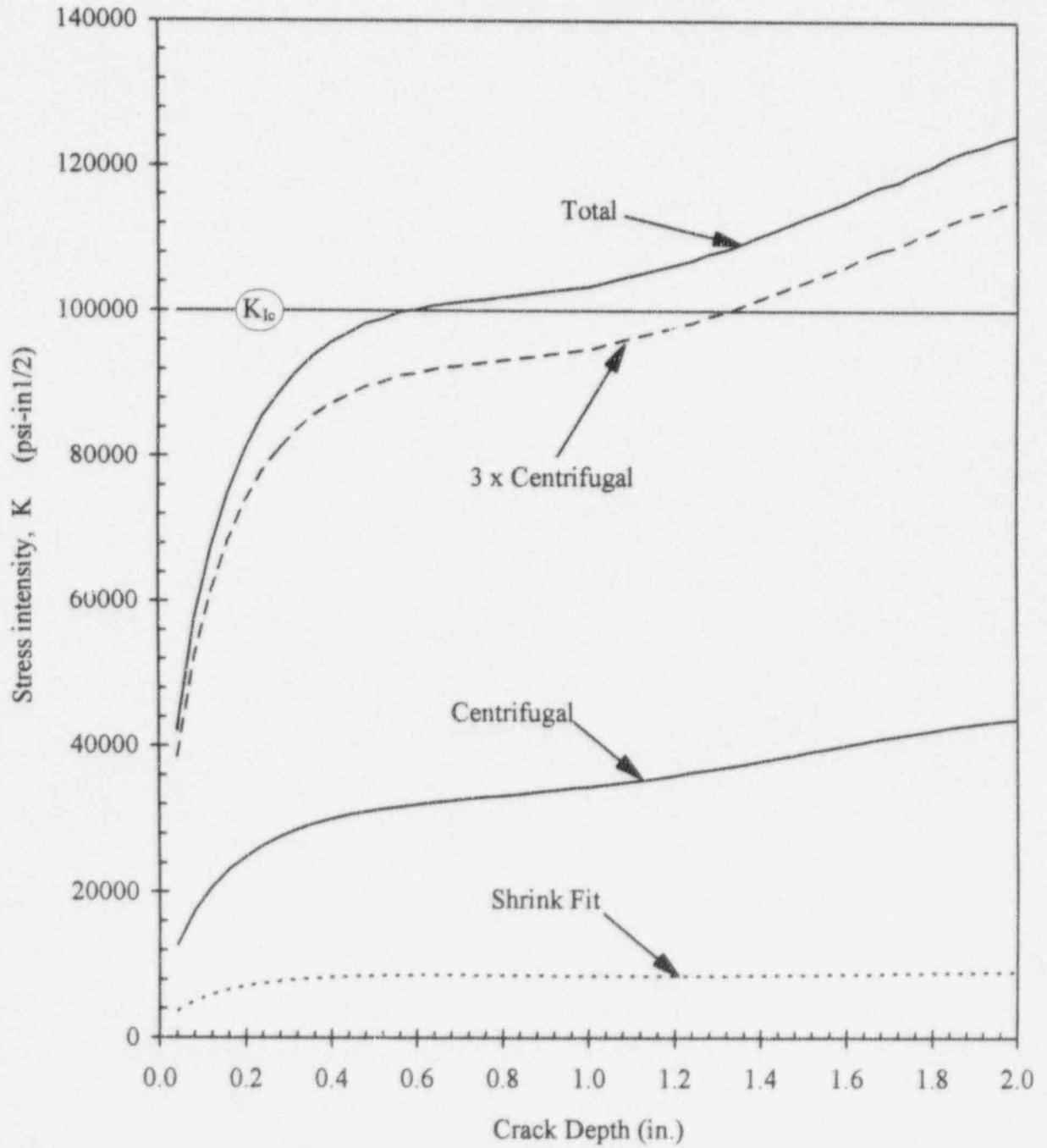


Figure 12. Determination of Allowable Flaw Size ($t/R = \infty$) - Waterford-3

Allowable Flaw Size Evaluation Normal Operating Conditions Small Bore - ANO-2

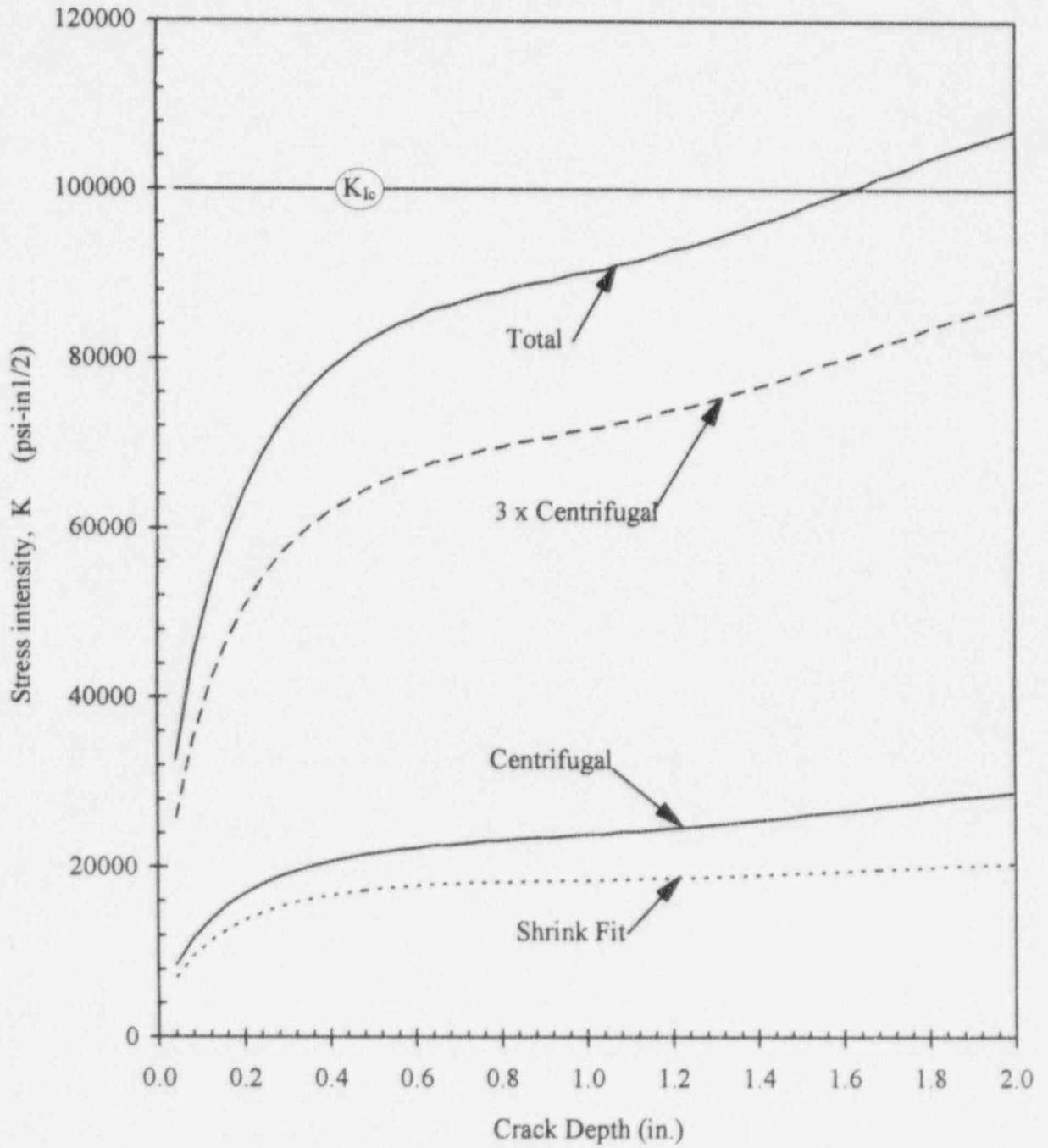


Figure 13. Determination of Allowable Flaw Size ($t/R = 1.2$) - ANO-2

Allowable Flaw Size Evaluation Normal Operating Conditions MILLSTONE

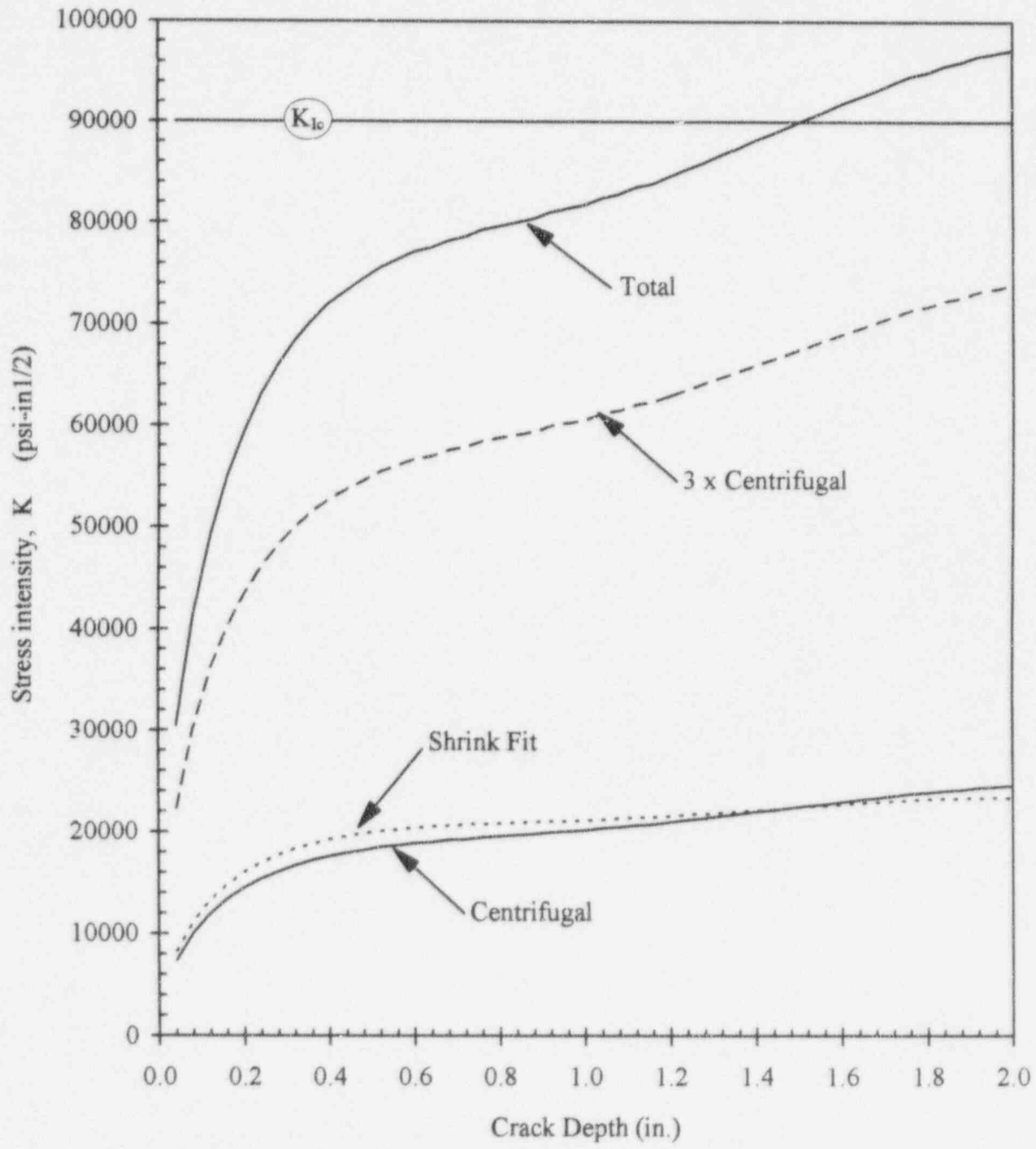


Figure 14. Determination of Allowable Flaw Size ($t/R = 1.2$) - Millstone-2

Allowable Flaw Size Evaluation Normal Operating Conditions WATERFORD

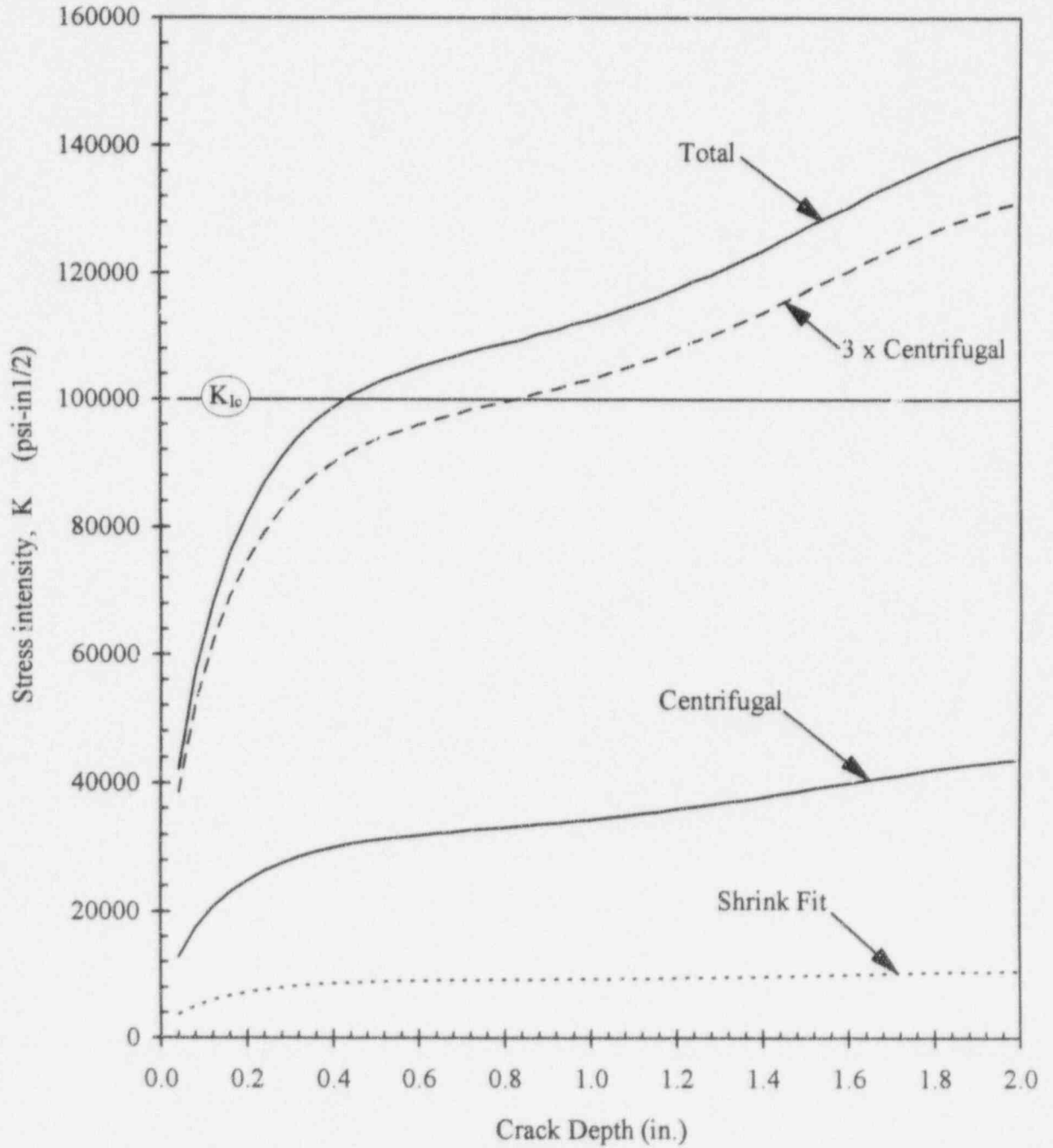


Figure 15. Determination of Allowable Flaw Size ($t/R = 1.2$) - Waterford-3

6. Provide information on the remaining shrink fit for accident conditions for all flywheels.

The estimated remaining shrink-fit for accident conditions for all flywheels is shown in Table 4. These were calculated by determining the centrifugal displacement at accident conditions and subtracting it from the initial shrink-fit.

**Table 4
 Remaining Shrink-fit at Accident Conditions**

Plant Name	Initial Shrink-Fit (in)	Centrifugal Displacement (in)	Remaining Shrink-Fit (in)
ANO-1	0.0125	0.0108984	0.00160
ANO-2	0.0052	0.003777	0.00142
Millstone-2	0.0052	0.003134	0.00207
Palisades	0.0125	0.006527	0.00597
St. Lucie 1 & 2	0.0125	0.006419	0.00606
Waterford-3	0.0052	0.005844	0.00000

7. Provide past RCP flywheel maintenance records in terms of maintenance frequency and level of disassembly involved.

Complete access to the flywheels allowing for a more thorough inspection is made possible during reactor coolant pump motor replacement evolutions. The historical motor replacements that have occurred at ANO are provided in Table 5 below.

**Table 5
 Historical Reactor Coolant Pump Motor Replacements at ANO**

ANO Unit	Pump	Type of Motor	Outage	Date
1	P32B	New	1R12	Spring 1995
2	2P32A	New	2R9	Fall 1992
2	2P32B	Refurbished	2R10	Spring 1994

The tentative ANO schedule for future reactor coolant pump motor replacements is provided in Table 6 below.

Table 6
Planned Future Reactor Coolant Pump Motor Replacements

ANO Unit	Pump	Type of Motor	Outage	Date
1	P32C or P32D	Refurbished	1R14	Spring 1998
1	P32C or P32D	Refurbished	1R15	Spring 2000
1	P32A	Refurbished	1R16	Spring 2002
2	2P32C	Refurbished	2R12	Spring 1997
2	2P32D	Refurbished	2R13	Spring 1999

8. Discuss the test results from the initial examination on Arkansas Nuclear One, Unit 1's RCP flywheels in terms of detection and sizing capability of the acoustic emission methodology used and the future inspection plan for these flywheels.

Acoustic-emission inspection involves the detection of released strain initially stored in a strain field. Detection forms the basis for analyzing the integrity of the material or structure. If a discontinuity is unstable and is affected by loading, the discontinuity will emit acoustical energy, which will reveal its presence. If the discontinuity is not affected by loading, it will not be an active emitter; that is, it is in a stable condition and will not affect the structural integrity of the material being tested.

In January 1983, acoustic emission tests were performed on reactor coolant pump motor flywheels P32A, P32B, P32C, and P32D at ANO-1. The evaluations of the four flywheels were accomplished in accordance with ANO test procedures.

The acoustic emission inspection system provided two independent analysis routines. Real-time Source Display (RSD) analyzes all emission intensities on a video screen which contains a geometrical layout of the structure being inspected. Source analysis computer (SAC) processes and analyzes emission data using criteria that selects only the predominantly (non-random) sources to analyze for structural location and significance.

The flywheel inspections were divided into two tests (Test 1 and Test 2). The inspection portions of Test 1 and Test 2 utilized the two independent analysis routines, RSD and SAC.

During Test 1, all flywheels showed random emissions during the RSD analysis. The random emissions were primarily in the region of the highest expected stress of the flywheels. All four flywheels released energy at a constant rate and at a low value indicating no Grade A sources (sources were insignificant to structural integrity). Neither predominant nor persistent emitters were detected on any of the four flywheels.

To confirm and correlate the results of the RSD analysis, post-test statistical computer analysis was conducted. The post test analysis revealed between one to three areas of source location correlation between transducer sets or stress increments. However, the data from these correlated areas did not meet the minimum grading criteria as defined in AEI-82-154, Rev. 1, Section 7.4 of Appendix A. Because the minimum grading requirements were not met, all of the identified areas of sources locations were classified as either innocuous, or minor and insignificant to structural integrity.

Test 2 of flywheels P32A, P32B, P32C, and P32D from the RSD revealed no predominant nor persistent emitters. On P32A, P32B and P32D only random emissions were detected from the regions of highest stress. On P32C mostly random emissions were displayed coming from the regions of highest stress and from the shaft and spoke region. The four flywheels had energy release rates that remained low, and no gradable sources were revealed in the post-test statistical computer analysis.

The most significant sources of emissions of the flywheel inspections were determined to be paint-to-metal interface, metal-to-metal interface of the flywheel, and bolted counterweight below the flywheel. The acoustic emission system is sensitive to sound both on and within the structure being tested. The majority of sounds transmitted during the two tests were of long duration such as those generated by structural interfaces moving with respect to each other, whereas, crack generation emissions are characteristic of short duration. The flywheel inspections did not reveal any indications of significance. All flywheels analyzed were of good integrity under the conditions imposed during the acoustic emission tests.

Acoustic emission crack detection is dependent on crack growth and deformation time. Acoustic emission is capable of detecting microcracks in the size range of 10^{-5} to 10^{-6} inches as they are formed. Increments of macrogrowth of the same dimension can also be detected. Crack growth that causes a motion in the sensor of 10^{-12} inches can be detected, assuming the deformation time is 20 microseconds or less. The sensitivity of the acoustic emission system can range from gross deformations, which cause audible sound, to micro-occurrences, such as movement of dislocations.

Acoustic emission is no longer utilized for the flywheel inspections at ANO-1. All four flywheels have been ultrasonically examined since the performance of the acoustic emission inspection. Future flywheel inspections at ANO-1 will continue to utilize ultrasonic techniques as the primary means of examination.